Epigenetics 8:5, 512–521; May 2013; © 2013 Landes Bioscience

Chromatin remodeling of human subtelomeres and TERRA promoters upon cellular senescence

Commonalities and differences between chromosomes

Peter E. Thijssen,[1,2] Elmar W. Tobi,[2] Judit Balog,[1] Suzanne G. Schouten,[2] Dennis Kremer,[2] Fatiha El Bouazzaoui,[1] Peter Henneman,[1,†] Hein Putter,[3] P. Eline Slagboom,[2] Bastiaan T. Heijmans[2,4] and Silvère M. van der Maarel[1,*]

[1]Department of Human Genetics; Leiden University Medical Center; Leiden, The Netherlands; [2]Department of Molecular Epidemiology; Leiden University Medical Center; Leiden, The Netherlands; [3]Department of Medical Statistics; Leiden University Medical Center; Leiden, The Netherlands; [4]Netherlands consortium for healthy ageing; Leiden University Medical Center; Leiden, The Netherlands

[†]Current affiliation: Department of Clinical Genetics; Academic Medical Center; University of Amsterdam; Amsterdam, The Netherlands

Keywords: chromatin remodeling, subtelomere, senescence, cellular aging, TERRA transcripts, histone modifications

Abbreviations: TERRA, telomere repeat containing RNA; SA β-gal, senescence associated β-galactosidase; SAHF, senescence associated heterochromatic foci; MEFs, mouse embryonic fibroblasts; FSHD, facio scapulo humeral muscular dystrophy; TSS, transcriptional start site; HDACs, histone deacetylase complexes; TRF, terminal restriction fragment

Subtelomeres are patchworks of evolutionary conserved sequence blocks and harbor the transcriptional start sites for telomere repeat containing RNAs (TERRA). Recent studies suggest that the interplay between telomeres and subtelomeric chromatin is required for maintaining telomere function. To further characterize chromatin remodeling of subtelomeres in relation to telomere shortening and cellular senescence, we systematically quantified histone modifications and DNA methylation at the subtelomeres of chromosomes 7q and 11q in primary human WI-38 fibroblasts. Upon senescence, both subtelomeres were characterized by a decrease in markers of constitutive heterochromatin, suggesting relative chromatin relaxation. However, we did not find increased levels of markers of euchromatin or derepression of the 7q *VIPR2* gene. The repressed state of the subtelomeres was maintained upon senescence, which could be attributed to a rise in levels of facultative heterochromatin markers at both subtelomeres. While senescence-induced subtelomeric chromatin remodeling was similar for both chromosomes, chromatin remodeling at TERRA promoters displayed chromosome-specific patterns. At the 7q TERRA promoter, chromatin structure was co-regulated with the more proximal subtelomere. In contrast, the 11q TERRA promoter, which was previously shown to be bound by CCCTC-binding factor CTCF, displayed lower levels of markers of constitutive heterochromatin that did not change upon senescence, whereas levels of markers of facultative heterochromatin decreased upon senescence. In line with the chromatin state data, transcription of 11q TERRA but not 7q TERRA was detected. Our study provides a detailed description of human subtelomeric chromatin dynamics and shows distinct regulation of the TERRA promoters of 7q and 11q upon cellular senescence.

Introduction

The last decade has provided deeper knowledge on the stability and maintenance of the repetitive telomeric repeat structures at the ends of human chromosomes in biological processes such as cellular senescence. Non-transformed cells derived from mitotic tissues have a limited proliferative capacity, known as the Hayflick limit,[1] and will eventually become senescent. Senescent cells exit the cell cycle, start secreting specific proteins that affect the microenvironment and display a number of senescence-associated markers, e.g., induction of cell cycle inhibitory proteins, senescence associated β-galactosidase (SA β-gal) and senescence associated heterochromatic foci (SAHF) formation.[2] Cellular senescence is considered an anti-tumorigenic mechanism which in vivo may be relevant especially at higher ages, since senescent cells accumulate with age in tissues with high cell turnover. In vitro, it has been shown that progressive shortening of telomeres is a potent trigger to induce cellular senescence.[3-5]

Telomeres constitute the terminal structures of eukaryotic chromosomes and form a protective barrier against the incomplete replication of linear DNA. In mammals, telomeres are comprised of simple (TTAGGG)n repeats folded into a heterochromatic loop structure, facilitated by the shelterin protein complex.[6] Numerous reports on the inverse correlation of telomere length in peripheral blood cells and donor age, age-related traits and the risk for various age-related diseases highlight the

*Correspondence to: Silvère M. van der Maarel; Email: S.M.Maarel@lumc.nl
Submitted: 01/21/13; Revised: 03/22/13; Accepted: 03/26/13
http://dx.doi.org/10.4161/epi.24450

potential relevance of telomere regulation.[7-11] It is as yet not clear, however, whether telomere shortening causally contributes to these traits or represents a marker of cell division and senescence.

Although most studies on the relationship between telomere shortening and senescence focused on its potential direct consequences on chromosome stability, it may have downstream consequences, particularly on the subtelomere, that may in turn affect telomere function.[12,13] Subtelomeres, the first non-TTAGGG sequences directly adjacent to the telomere repeat, are evolutionary conserved chromosome domains consisting of patchworks of sequence blocks with high inter- and intrachromosomal similarity.[14,15] Subtelomeres are packed into constitutive heterochromatin, characterized by high levels of histone 3 lysine 9 trimethylation (H3K9me3) and CpG methylation.[13] A steep decrease of both markers is seen at subtelomeres upon drastic telomere shortening in mouse embryonic fibroblasts (MEFs) isolated from telomerase deficient mice, concomitant with an increase of markers for euchromatin (histone acetylation). This indicates a relative opening of the chromatin template at subtelomeres upon telomere shortening.[12,13]

Several human studies focusing on aging, as well as age related disease like Parkinson and Alzheimer disease, showed that telomere length correlates with CpG methylation at subtelomeres and that the direction of this correlation is dependent on the disease conditions.[16-18] A recent study in dyskeratosis congenita suggested an interaction between the proper maintenance of telomeres and the chromatin state of subtelomeres.[19] A more causal relation between dysregulation of subtelomeric chromatin and human disease is seen in the progressive muscular dystrophy facioscapulohumeral muscular dystrophy (FSHD). In FSHD, decreased chromatin compaction by reduced levels of CpG methylation and H3K9me3 at the subtelomeric D4Z4 repeat, encoding the toxic DUX4 protein, leads to its aberrant transcription in muscle.[20-22]

Chromatin alterations at subtelomeres may have other direct transcriptional consequences, as they harbor transcriptional start sites (TSS) for telomeric repeat containing RNAs (TERRA).[23] The transcription of these long non-coding RNAs is influenced by subtelomeric CpG methylation and myeloid/lymphoid or mixed lineage leukemia (MLL) mediated H3K4me3.[24,25] More recently, a role for CTCF and cohesin was established in controlling telomeric transcription.[26] Telomere elongation by ectopic expression of telomerase, represses TERRA transcript levels and leads to increased levels of telomeric H3K9me3 without a concomitant change in the subtelomeric chromatin state.[27] In yeast, recent data shows that inducing TERRA expression leads to accelerated telomere shortening, by facilitating exonuclease activity at transcribed chromosome ends.[28,29]

From the currently available data a feedback model is emerging in which telomere length regulates the epigenetic structure of subtelomeres, thereby possibly affecting TERRA expression levels, which in turn have an effect on telomere length, induction of senescence and chromatin state. The data supporting this model were obtained in diverse model systems, using ectopic telomere length modulation or TERRA regulation. However, chromosome-specific data on subtelomeric chromatin remodeling and TERRA promoter regulation upon cellular senescence by physiological telomere shortening in a human system is lacking. Therefore, we systematically interrogated the chromatin state of subtelomeres in senescing primary human WI-38 fibroblasts. The chromatin state was assessed by quantifying markers for euchromatin (histone acetylation) and constitutive (CpG methylation, H3K9me3) and facultative (H3K27me3, H3K36me3) heterochromatin along the subtelomere. Together with chromosome specific analysis of TERRA promoters and transcripts, a complex picture of both common and chromosome specific epigenetic changes at human subtelomeres upon cellular senescence emerges.

Results

Late passage WI-38 fibroblasts display a senescent phenotype. To study subtelomere chromatin dynamics upon cellular senescence, we cultured WI-38 fibroblasts until they reached a senescent phenotype. Upon senescence, we observed overall telomere shortening evidenced by a shift in the smear in a TRF analysis (**Fig. 1A**). Subsequent qPCR analysis revealed a 65% reduction in telomere copy number comparing early passage cycling cells to late passage senescent cells (E vs. L, **Fig. 1B**). Upon cellular senescence, expression of the cell cycle inhibitory protein p16 was induced approximately 2 fold (**Fig. 1C and D**). Moreover, we observed that late passage cells display high levels of SAβ-gal activity in more than 95% of the cells, whereas in early passage only sporadic cells show staining (**Fig. S1**). Taken together, late passage WI-38 fibroblasts underwent replication induced telomere shortening and showed a senescent phenotype, in contrast to early passage cells.

Decrease in markers of constitutive heterochromatin at subtelomeres upon senescence. The subtelomeres of human chromosome arms 7q and 11q are consisting of a single copy sequence which facilitates a chromosome specific analysis of histone modification levels at multiple loci with increasing distance to the telomere (**Fig. 2A**). We assessed H3K9me3 levels at six loci on both subtelomeres and observed a variable 2–3 fold decrease of this modification at all loci upon cellular senescence (**Fig. 2B and C**). The decrease of H3K9me3 was not detected at the repressed, non-subtelomeric CT47 macrosatellite repeat array,[30] arguing against a general loss at heterochromatic loci (**Fig. S2A**). At the promoter of the actively transcribed *GAPDH* gene, no change in the low level of H3K9me3 was observed upon cellular senescence (**Fig. S2B**).

Mean methylation levels of sporadic CpGs at the regions under study showed variable levels at different loci, but at 4 out of 5 tested loci a significant decrease of 8–17% upon senescence ($p < 0.05$) was observed (**Fig. 2D and E**). The 5th locus, at 10 kb from the 11q telomere, showed a similar trend ($p = 0.08$). Analysis of individual CpGs supported this observation (**Fig. S3**). Analysis per chromosome, by calculating the mean methylation level over multiple amplicons, revealed a significant average decrease of ~10% at 7q and ~6% at 11q ($p < 0.05$, **Fig. 2F**). Overall, we observed a reduction in markers of constitutive heterochromatin at two human subtelomeres upon

cellular senescence, indicating a relative opening of the chromatin template.

No increased levels of euchromatin markers at subtelomeres upon senescence. In Terc$^{-/-}$ mice MEFs, the decrease of markers of constitutive heterochromatin with drastic telomere shortening is accompanied by increased histone acetylation levels.[12] In our human cell system, H3K9ac was virtually absent at subtelomeres both in the early passage and upon cellular senescence (**Fig. S4**). In contrast, H4K16ac was detected, but a decrease of at least 2 fold (**Fig. 3A and B**) was observed upon senescence. The latter was however not restricted to subtelomeres, as we observed a comparable decrease of this modification at the heterochromatic CT47 macrosatellite repeat array (**Fig. S2A**). In the context of the promoter of the actively transcribed GAPDH locus a relatively small increase of H4K16ac was observed (**Fig. S1B**). Altogether, we did not find evidence that the decreased levels of constitutive heterochromatin markers at subtelomeres upon senescence are accompanied by increased levels of markers of euchromatin.

Increased levels of H3K27me3 and H3K36me3 may compensate for loss of markers of constitutive heterochromatin. We wondered why the decrease of markers of constitutive heterochromatin marks did not go together with an increased level of euchromatin marks. Therefore, we tested whether chromatin repression was actually maintained, by involvement of different repressive mechanisms instead. As the Polycomb mediated H3K27me3 is considered a marker for both facultative and constitutive heterochromatin, we assessed its levels at the subtelomeres upon senescence. H3K27me3 was indeed detected at subtelomeres in early passage cells and we observed an up to 2 fold increase of this modification upon cellular senescence at 7 out of 12 loci on 7q and 11q (**Fig. 3C and D**). This suggests that a Polycomb-enforced chromatin repression occurs at these loci upon cellular senescence. The increase of H3K27me3 was most pronounced at 250 kb from the telomere on chromosome 7q, which is located in the fourth intron of the *VIPR2* gene. Transcripts emanating from this gene were not detected in both passages (data not shown), again indicating the repressed chromatin state is indeed preserved in senescing cells. At the heterochromatic CT47 macrosatellite repeat array and the euchromatic *GAPDH* promoter we did not see increased levels of H3K27me3 (**Fig. S2**).

Recently it was shown that H3K36me3, a marker associated with actively transcribed gene bodies, is associated with both facultative and constitutive heterochromatin regions in mouse.[31] At the subtelomeres of 7q and 11q, we detected H3K36me3 with an increase of at least 2 fold upon senescence at both subtelomeres (**Fig. 3E and F**). All subtelomeric loci displayed higher levels of this marker, but the largest increase was again detected within VIPR2. Increased H3K36me3 was not restricted to subtelomeres, as similar increases were detected at the GAPDH promoter and CT47 macrosattelite repeat array (**Fig. S2**). Taken together, these data suggest a relative opening by reduction of constitutive heterochromatin markers is accompanied by increased levels of two heterochromatin markers associated with different repressive

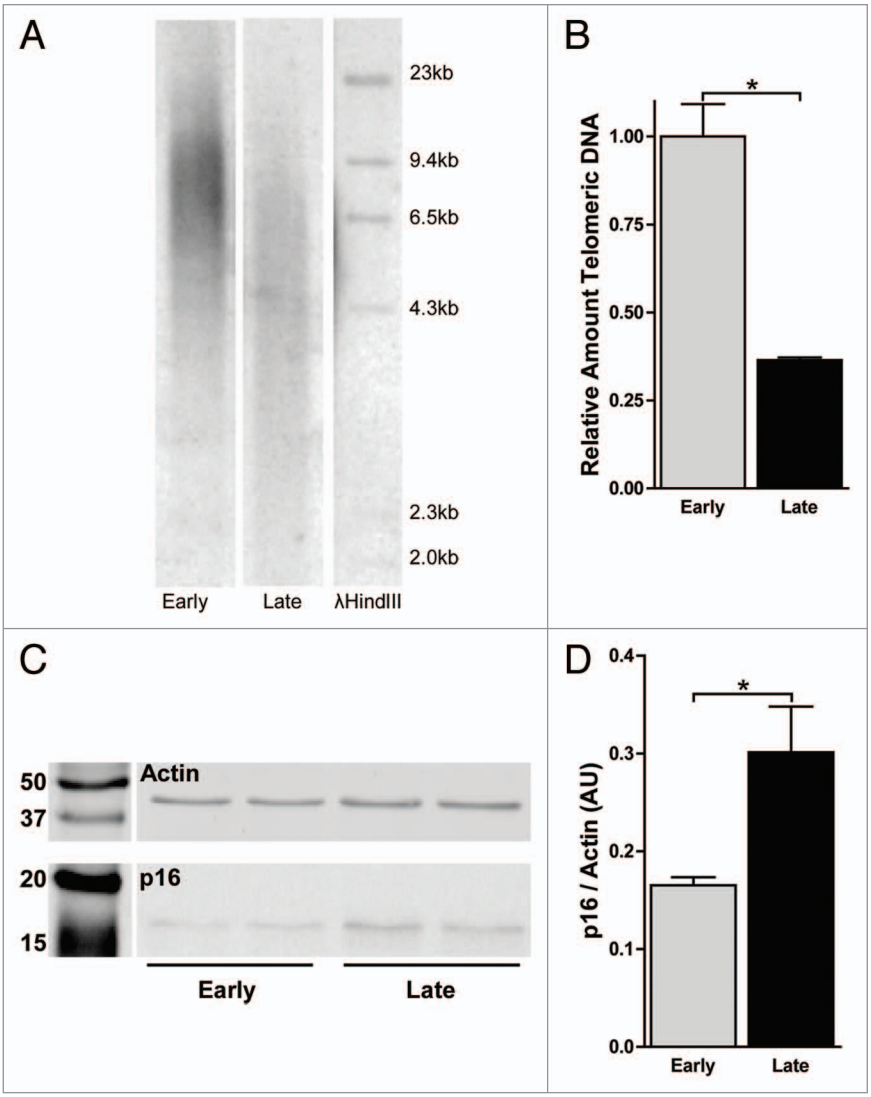

Figure 1. Late passage WI-38 fibroblasts underwent telomere shortening and display a senescent phenotype. (**A**) TRF analysis on genomic DNA isolated from early (E) passage and late (L) passage cells. DNA was digested with RsaI and AluI and reduction of the average telomere length is seen by the shift in the smear of the undigested telomeric DNA. (**B**) Normalized relative quantification of telomeric copy number in E and L passage cells. Telomeric copy number was quantified by qPCR, relative to the *36B4* single copy locus and normalized to E passage cells. Error bars indicate SEM of a triplicate measurement. (**C**) Western blot analysis in of p16 and actin expression in E and L passage cells followed by (**D**) relative quantification, showed increased expression of p16 in L passage cells. Error bars indicate stdev of two biological replicates, asterisks indicate a p-value < 0.05 based on a Student's t-test.

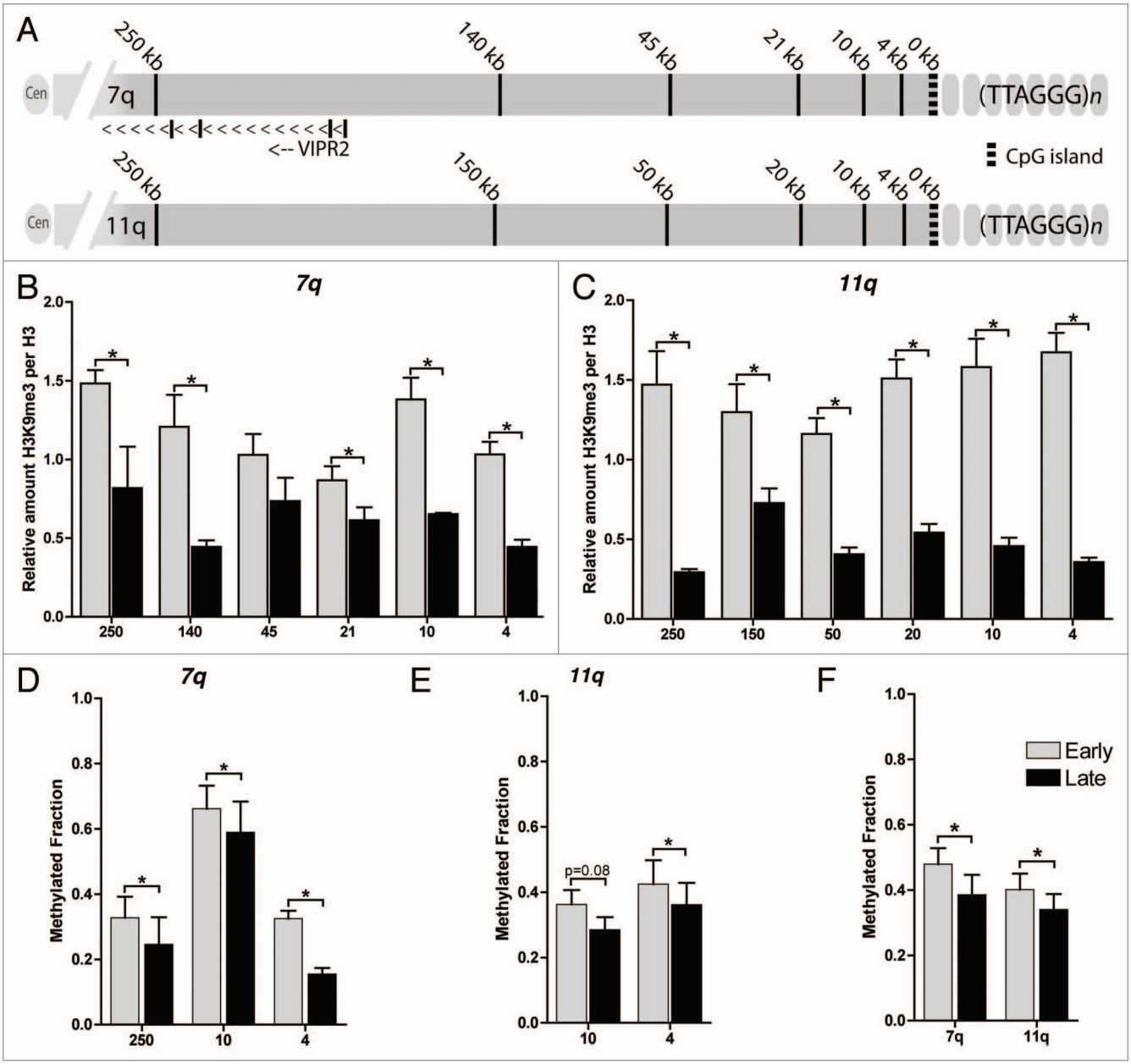

Figure 2. Decreased levels of markers of constitutive heterochromatin at subtelomeres upon senescence. (**A**) Location of the generated primer pairs along the subtelomeres of chromosome 7q and 11q. (**B**) Relative quantification using ChIP-qPCR of H3K9me3 along the subtelomeres of 7q and (**C**) 11q shows a decrease at all loci upon senescence. H3K9me3 levels are corrected for IgG background and normalized to the relative amount of H3: $(Ct_{IgG} - Ct_{H3K9me3})/(Ct_{IgG} - Ct_{H3})$. Error bars indicate SEM of at least duplicate qPCR measurements, asterisks indicate a p-value < 0.05 based on a student's t-test. (**D**) EpiTYPER based quantification of CpG methylation along the subtelomere of 7q and (**E**) 11q showed a decreased DNA methylation at all sites measured. The mean methylation of multiple CpGs within the indicated probes is displayed. (**F**) Combined mean methylation levels of all subtelomeric probes at 7q and 11q showed a decreased DNA methylation along both subtelomeres. DNA methylation was quantified in triplicate, p-values are indicated and * indicates a p-value < 0.05 based on UNIANOVA analysis.

mechanisms, which may maintain the repressed subtelomeric chromatin state upon senescence.

Since both model subtelomeres under study are of single copy nature, we wondered to what extent the observed effects would apply to other, more repetitive subtelomeric loci. To that end, we measured relative abundance of histone modifications at D4Z4, a subtelomeric repeat structure present at chromosomes 4q and 10q, that has been extensively studied in the context of FSHD.[21] This showed that the described chromatin remodeling occurs on other subtelomeres as well, as we observed similar changes upon senescence compared with the subtelomeres of 7q and 11q (**Fig. S5**).

Specific chromatin regulation of 7q and 11q TERRA promoters upon senescence. The distal ends of subtelomeres harbor the TSS of TERRA transcripts. Recent data showed the involvement of the insulator protein CTCF at the TERRA promoter of

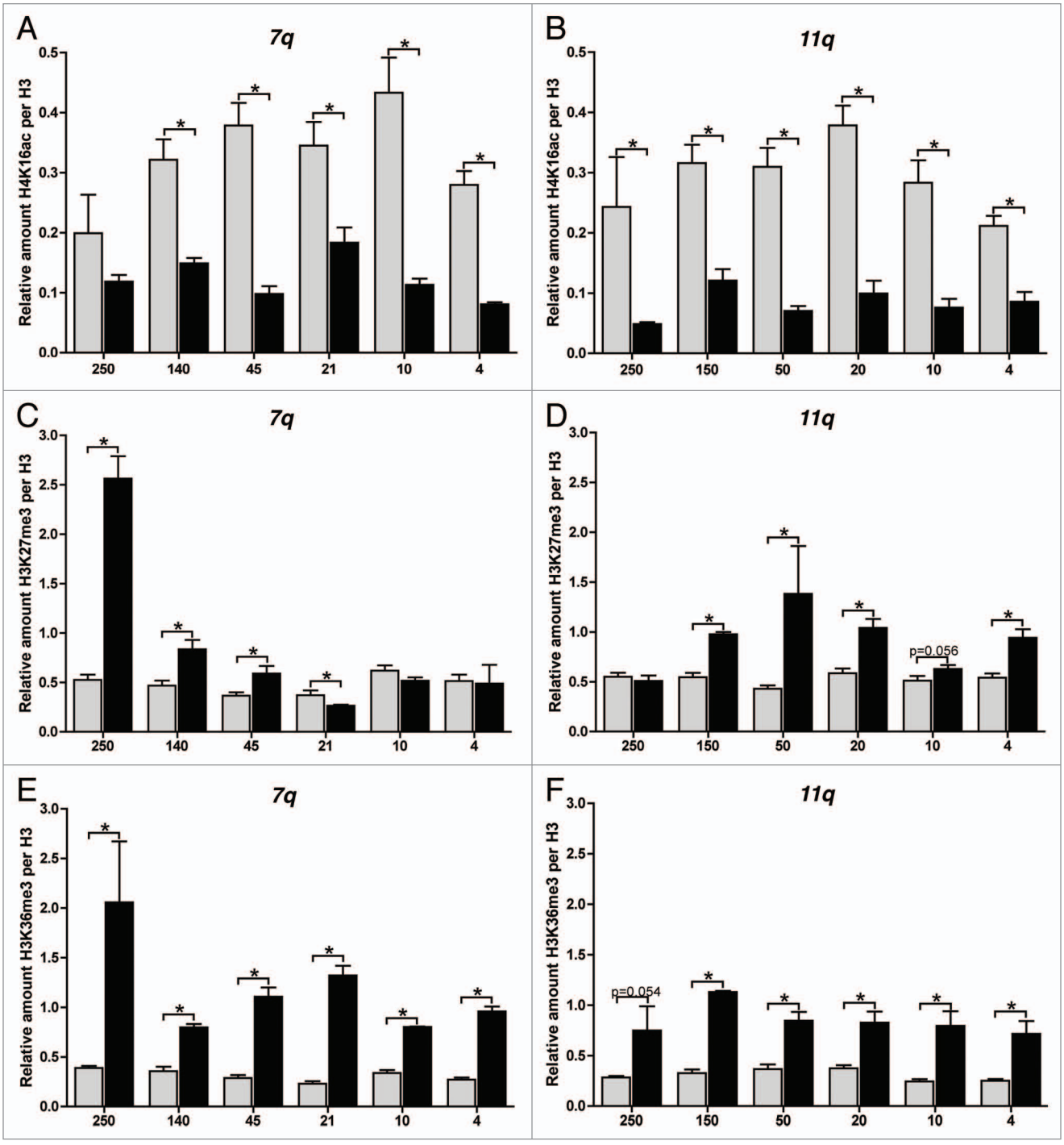

Figure 3. Relative quantification of subtelomeric H4K16ac, H3K27me3 and H3K36me3 upon senescence. Relative quantification using ChIP-qPCR of H4K16ac (**A and B**), H3K27me3 (**C and D**) and H3K36me3 (**E and F**) at increasing distance from the telomere at the subtelomeres of 7q (**A, C and E**) and 11q (**B, D and F**). H4K16ac is decreased at all loci and H3K36me3 shows an increase at both subtelomeres. H3K27me3 shows a more varied pattern; an increase is observed at 7 out of 12 loci. All values are corrected for IgG background and normalized to the relative amount of H3 $[(Ct_{IgG} - Ct_{modification})/(Ct_{IgG} - Ct_{H3})]$, error bars indicate SEM of duplicate qPCR measurements, asterisks indicate a p-value < 0.05 based on a student's t-test.

11q, but not at 7q.[26] Indeed, querying the WI-38 CTCF ChIP-seq tracks available from the UCSC genome browser, revealed CTCF binding just proximal to the TERRA promoter site at 11q, but not at 7q. We sought evidence for transcriptional activity of 7q and 11q TERRA in our cell system. Both in early passage and senescent cells we detected 11q TERRA transcripts, however, we could not detect TERRA transcripts emanating from 7q in both cell passages (**Fig. 4A**). Previously identified Xq transcripts[24] were detected in both early and late passage cells and served as a control (**Fig. 4A**).

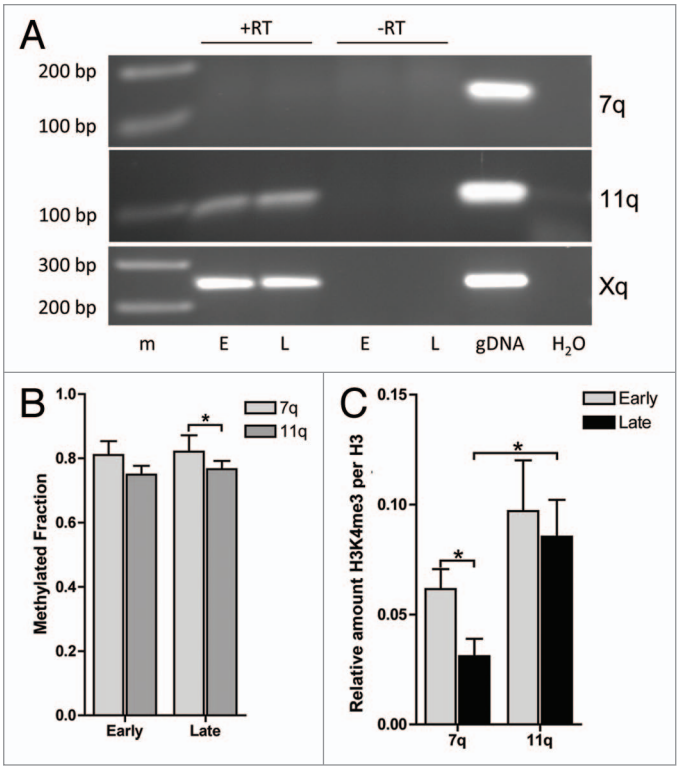

Figure 4. TERRA promoter analysis reflects transcriptional activity at 7q and 11q irrespective of senescence. (**A**) RT-PCR analysis of 7q, 11q and Xq specific TERRA transcripts allowed detection of 11q, but not 7q specific transcripts. Xq serves as an internal control. –RT: cDNA synthesis in the absence of reverse transcriptase to control for DNA background. gDNA: positive control for the PCR on a WI-38 genomic DNA extract. (**B**) Epityper based quantification of TERRA promoter CpG methylation at 7q and 11q showed higher levels of methylation at 7q pTERRA compared with 11q pTERRA. The mean methylation of multiple CpGs within the indicated probes is displayed. Upon senescence TERRA promoter methylation at both 7q and 11q does not change. Indicated p-values (* < 0.05) were obtained using an UNIANOVA analysis of triplicate measurements. (**C**) Relative quantification by ChIP-qPCR of H3K4me3, marking active promoters, showed higher levels at 11q pTERRA compared with 7q pTERRA, irrespective of senescence. All values are corrected for IgG background and are normalized to the relative amount of H3 ($Ct_{IgG} - Ct_{H3K4me3}$)/($Ct_{IgG} - Ct_{H3}$). Error bars indicate SEM of duplicate qPCR measurements, asterisks indicate a p-value < 0.05 based on a student's t-test.

In line with this, the mean DNA methylation in senescent cells at the CpG dense TERRA promoter of 7q showed a significantly ($p < 0.05$) higher methylation level than its 11q counterpart (~81% at 7q vs. ~75% at 11q). Although not significant, we observed a similar trend in early passage cells (**Fig. 4B**). Moreover, promoter-associated H3K4me3 levels, previously shown to be involved in TERRA regulation,[25] were 40–60% lower at 7q compared with 11q (**Fig. 4C**). Global TERRA levels are reported to decrease upon senescence,[25] which is in line with lower abundance of H3K4me3 at both 7q and 11q (**Fig. 4C**). CpG methylation levels did not change upon senescence, although some individual CpGs changed in both directions (**Fig. S6**).

To further determine the chromatin regulation of the TERRA promoters upon senescence, we quantified histone modification levels at both 7q and 11q. 7q pTERRA displayed similar chromatin dynamics upon senescence as the more proximal 7q subtelomere: reduced H3K9me3 and H4K16ac levels with an increase of H3K36me3 upon senescence. H3K27me3 showed a small decrease, however the described increase of this mark was mostly seen at greater distance to the telomere (**Fig. 5A–D**).

In contrast, at 11q, bound by CTCF, we observed differential regulation of pTERRA compared with the proximal subtelomere. In early passage cells, the relative amount of H3K9me3 at pTERRA (1.04) was lower compared with more proximal sites (~1.44 on average), but we did not observe a decrease upon senescence (**Fig. 5A**). Strikingly, H3K27me3 showed a 2-fold decrease upon senescence, contrary to the more proximal subtelomere, where a change in opposite direction was observed (**Fig. 5C**). H4K16ac and H3K36me3 levels at pTERRA are comparable to the more proximal sites, although the levels of both markers remained higher upon senescence (**Fig. 5B and D**). Altogether, we observed that upon senescence, the chromatin remodeling of the 7q TERRA promoter is similar to the proximal subtelomere. The TERRA promoter at 11q however, showed a distinct chromatin remodeling upon senescence when compared with the proximal 11q subtelomere.

Discussion

In this study, we systematically interrogated the changes in chromatin structure of human subtelomeres upon cellular senescence. Previous studies, in which ectopic telomere length modulation resulted in a large contrast in telomere length, reported opposing data on the effect of telomere length, a known trigger for cellular senescence, and subtelomeric chromatin state.[12,27] In our model, using primary human fibroblasts, we observed a senescence-associated reduction of constitutive heterochromatin markers, which is accompanied by a gain of facultative repressive marks. Our data indicate that the repressed state is preserved during senescence as we found no increased levels of markers of euchromatin or evidence for derepression of the only annotated gene in the studied region. Furthermore, we observed distinct regulation of two TERRA promoter sites at subtelomeres of 7q and 11q. These data complement with recent data showing the involvement of CTCF and cohesin in chromosome-specific epigenetic regulation of TERRA.[26]

Upon cellular senescence, we observed a decrease in two markers of constitutive heterochromatin, H3K9me3 and CpG methylation, suggesting a relative relaxation of the chromatin structure. Reduced levels of these markers at subtelomeres were previously reported upon drastic telomere shortening in MEFs of a telomerase deficient mouse model.[12] In contrast, telomere elongation by ectopic telomerase expression in human cell lines did not result in subtelomeric epigenetic changes.[27] However, the contrast in telomere length by ectopic telomerase expression is small, which may better reflect human physiological conditions, compared with telomerase deficient mice. Although the exact nature of the mechanism by which telomere length controls subtelomeric heterochromatin formation remains enigmatic, our data show that physiological telomere shortening and senescence

signaling result in decreased levels of constitutive heterochromatin marks at subtelomeres.

Upon reduced H3K9me3 and CpG methylation, a concomitant increase of markers of euchromatin (histone acetylation) is seen with drastic telomere shortening in *Terc*$^{-/-}$ MEFs.[12] In our model, we did not observe a similar effect upon senescence. H3K9ac levels were low in both passages and we observed decreased levels of H4K16ac upon cellular senescence. Subtelomeric H4K16ac was previously shown to be higher upon aging in yeast, as a consequence of reduced Sir2 expression.[32] Global H4K16 deacetylation, on the contrary, was shown to be involved in the DNA damage response and associates with cellular senescence of MEFs in a mouse model for the Hutchinson Gilford premature aging syndrome.[33] Our data show that the reduced levels of H4K16ac are not restricted to subtelomeres and are likely to be a genome-wide phenomenon, in concordance with its role in the DNA damage response and senescence.

We hypothesized that further chromatin activation upon decreased levels of markers of constitutive heterochromatin may be prevented by increased levels of the Polycomb-dependent repressive H3K27me3 modification. Both H3K9me3 and H3K27me3 were previously reported to change globally upon cellular senescence in human primary fibroblasts.[34] O'Sullivan et al. describe decreased H3K9me3 and increased H3K27me3 levels, which is in accordance with our observations at subtelomeres. Recent data, showing that the genome wide distribution of these markers does not change with RAS induced cellular senescence in human fibroblasts, suggest a different effect of oncogene induced compared with replicative senescence.[35]

H3K36me3 is mostly studied in the context of actively transcribed genes, but was recently suggested to be enriched in constitutive and facultative heterochromatin in mouse cells.[31] Indeed, we find considerable levels of this marker at both subtelomeres and at the silenced CT47 locus. In yeast, H3K36me3 recruits histone deacetylase complexes (HDACs) and thereby ensures repression of intragenic cryptic promoters.[36-38] It may be speculated that a similar mechanism exists in which subtelomeric sites become transcriptionally derepressed upon decreased levels of constitutive heterochromatin, eventually leading to deposition of H3K36me3 and recruitment of HDACs. In this scenario, higher levels of H3K36me3 have a repressive effect on the chromatin, maintaining the silenced state upon a decrease in H3K9me3 and CpG methylation. However, the increased H3K36me3 levels were not specific for subtelomeres and in our model we cannot disentangle the order of events to prove this concept. More understanding of the context dependent functionality of the H3K36me3 mark is therefore desired.

Subtelomere CpG methylation and histone modification levels have been subject of study in the context of several human diseases and aging. Throughout these studies, a positive correlation between telomere length and subtelomeric CpG methylation was observed, which was depended on different disease states and integrity of the telomere maintenance pathway.[16-19] Indeed, with reduced telomere length and induction of senescence we observed reduced levels of CpG methylation at subtelomere. In the progressive muscular dystrophy FSHD, the subtelomeric D4Z4 repeat array is characterized by reduced CpG methylation and H3K9me3 levels, compared with controls.[20-22] In FSHD cell

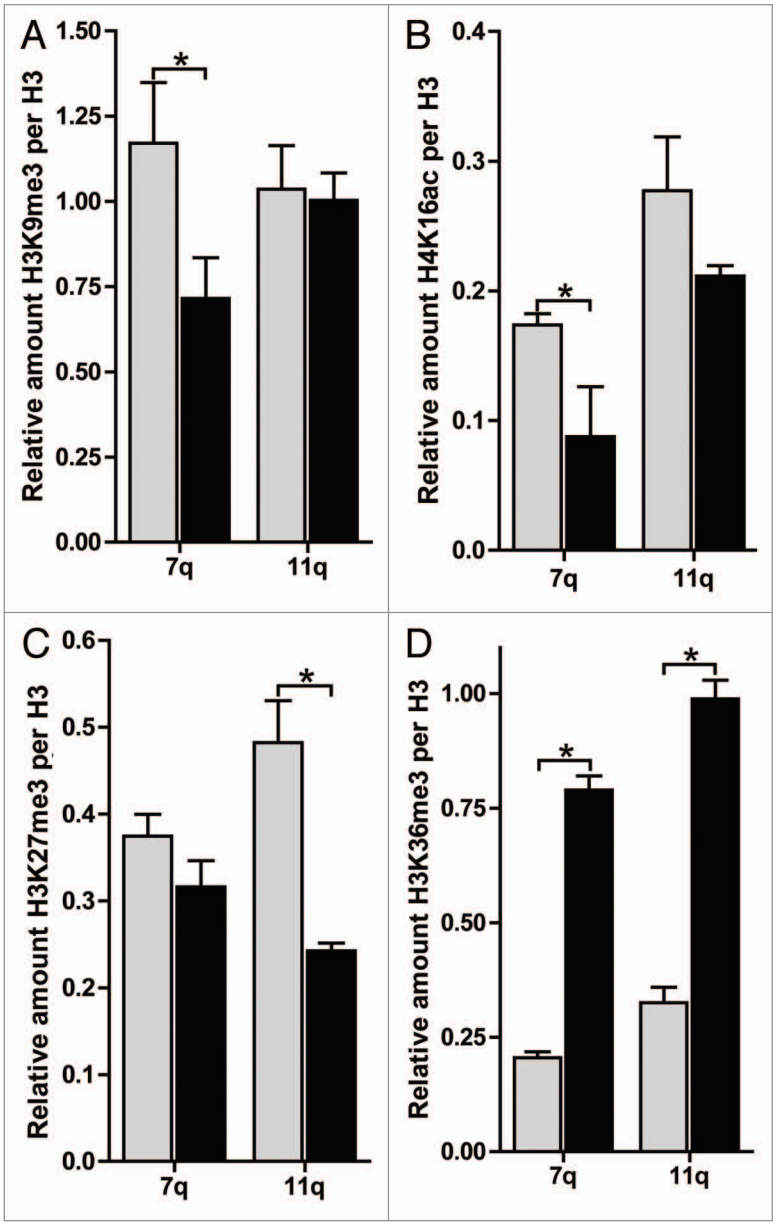

Figure 5. Distinct chromatin remodeling at TERRA promoters of 7q and 11q upon senescence. TERRA promoter analysis showed distinct regulation of (**A**) H3K9me3, (**B**) H4K16ac, (**C**) H3K27me3 and (**D**) H3K36me3 between 7q and 11q. The changes at the 7q TERRA promoter reflect the more proximal subtelomere, whereas the 11q TERRA promoter regulation is distinct from the more proximal subtelomere. All values are corrected for IgG background and are normalized to the relative amount of H3 [$(Ct_{IgG} - Ct_{modification})/(Ct_{IgG} - Ct_{H3})$]. Error bars indicate SEM of duplicate qPCR measurements, asterisks indicate a p-value < 0.05 based on a Student's t-test.

cultures, telomere length or senescence markers have not been studied. Our data may have implications for studying the epigenetic regulation of D4Z4, as we show that the replicative history of cell cultures can affect the chromatin structure of subtelomeres, also of the subtelomeric D4Z4 repeat array.

Since subtelomeres predominantly consist of repetitive sequences and subtelomeres of different chromosomes share highly homologous sequence blocks,[14,15] we selected the single copy subtelomeres of 7q and 11q as a model. This allowed us to systematically screen the subtelomere at increasing distance to the telomere to identify possible position effects. However, we did not find a clear relation between the distance to the telomere and the changes in subtelomeric chromatin structure. The observed chromatin changes at the subtelomeres of chromosomes 7q and 11q and the D4Z4 repeat array at 4q and 10q were highly similar and possibly reflect a general phenomenon of subtelomeric chromatin remodeling upon senescence. We cannot, however, rule out specific chromatin regulation at other subtelomeres or at different locations at the subtelomeres under study. Moreover, we have only studied the effect of senescence in a single model system for cellular senescence. To assess whether our observations are in general associated with senescence, additional models should be studied.

A striking exception to the commonalities between the studied chromosomes was the distinct regulation of the TERRA promoter at the subtelomeres of 7q and 11q. TERRA expression is regulated by specific CpG island motifs which have been identified on at least 20 different chromosome arms.[24] This specific CpG island is absent at both 7q and 11q, however CpG dense sequences are present just proximal to the telomere of both chromosomes. We demonstrated that DNA methylation at these CpG islands does not change upon senescence, in spite the fact that TERRA transcripts were shown to be downregulated upon senescence.[25] The H3K4 methyltransferase MLL has been shown to associate with telomeres and regulate TERRA transcription.[25] Low but detectable levels of H3K4me3 were detected at the TERRA promoters of 7q and 11q and we detected higher levels at 11q than at 7q, irrespective of senescence. Both CpG methylation and H3K4me3 levels are reflected in transcriptional activity, as we only could detect 11q transcripts. As TERRA has been shown to regulate telomere length, chromosome specific differences in TERRA regulation could offer an explanation for the observed allelic variation of telomere length in senescent human cells.[39]

Our data again emphasize that a chromosome arm specific analysis is needed considering the regulation of TERRA.[26] We showed that the 11q TERRA promoter is differentially regulated compared with the more proximal subtelomere, in contrast to the TERRA promoter of 7q. This is in line with recently published data, where involvement of CTCF and cohesin in TERRA regulation was shown at 11q, but not at 7q.[26] Next to its described role in TERRA transcription, our data suggests that the binding of CTCF proximal to the TERRA promoter results in the insulation and specific chromatin regulation of the TERRA promoter upon senescence. It may be hypothesized that TERRA promoters bound by CTCF, are be protected from the effects of telomere shortening and senescence signaling on the chromatin structure of subtelomeres, which would ensure proper regulation of TERRA transcription.

In conclusion, we show that human subtelomeres undergo extensive chromatin remodeling upon cellular senescence. A decrease in markers of constitutive heterochromatin does not lead to subtelomeric derepression but is accompanied by increased levels of transcriptional repressive modifications. We observed a strong overlap between the two subtelomeres under study, however, with respect to TERRA promoters, we showed chromosome specific remodeling occurs.

Materials and Methods

Cell culture and β-galactosidase assay. WI-38 human fetal lung fibroblasts at two different population doublings (15, early and 34, late) were obtained from Corriell (Corriell Cell Repositories). Early passage cells were expanded for 3–4 passages in DMEM F12 (31331) supplemented with 20% heat inactivated Fetal Calf Serum, 1% pen-strep, 1% sodium pyruvate and 1% HEPES (all Invitrogen Life Technologies) at 37°C, 5% CO_2. Senescent cells were obtained by expanding PDL 34 cells until a non-proliferative state was reached. Cells were then kept in culture for an additional period of 2–3 weeks and to confirm senescence, activation of β-galactosidase was assessed as described.[40] DNA, RNA, chromatin and protein were isolated in parallel. Both early passage and late passage cells were expanded, harvested and examined n three independent experiments of which one complete set is shown.

Protein isolation, western blot and quantification of p16. Cells were washed twice in 1 × PBS and after removal cells were lysed in RIPA buffer: 20 mM TEA, 0.14 M NaCl, 0.1% DOC, 0.1% SDS, 0.1% triton X-100, 1 × Complete EDTA free protease inhibitor cocktail and 1x Phosstop phosphatase inhibitor cocktail (both Roche) and sheared by passing through a 29G needle. Soluble protein content was measured by standard Pierce BCA analysis (Thermo Scientific) and 15 μg protein was loaded on a standard 15% SDS PAGE. After protein transfer, membranes were blocked and incubated o/n at 4°C with antibodies against p16 (1:500, sc-56330, Santa Cruz Biotechnology) and actin (1:1000, A2066, Sigma). Detection and relative quantification were done using the Odyssey system (V3.0, LI-COR Biosciences).

Telomere length analysis by Southern blot and qPCR. Genomic DNA was isolated using a standard salting out method. Southern blot based telomere length analysis was done as described before.[41] In brief, 3 μg genomic DNA was o/n digested with RsaI and AluI (Thermo Scientific) at 37°C and size separated on a 0.9% TAE agarose gel. DNA was denatured by incubating the gel in 0.4 M NaOH, 0.6 M NaCl for 30 min, nicked and crosslinked by UV light and subsequently transferred to a Hybond XL membrane (GE Healthcare). The membrane was hybridized, washed, scanned with a Storm 820 phosphorimager (GE Healthcare) and analyzed using imagequant software (v2003.03. GE Healthcare). qPCR analysis of telomeric copy number was done as described before[42] on the CFX96™ thermal cycler using iQ SYBR Green Supermix (both Bio-rad). Relative

telomere length was calculated using the single copy 36B4 locus as a reference and subsequently normalized using the CFX software (v2.0, Bio-rad).

Chromatin immunoprecipitation. ChIP experiments were based on the protocol described by Nelson et al. with some modifications.[43] In brief, cells were crosslinked in 1% formaldehyde (Merck-Milllipore) for 10 min and the reaction was quenched for five minutes in 125 mM glycine. Cross linked cells were lysed and chromatin was sheared in a sonicator bath (Bioruptor UCD-20, Diagenode) for four consecutive rounds of 10 min at maximum output and 15 sec on/off cycles. Shearing was analyzed by phenol-choloroform extraction of DNA and agarose gel electrophoresis. All chromatin samples had a DNA size range between 200–2,000 bp. Three μg (DNA amount) chromatin was precleared with blocked sepharose A beads (GE Healthcare) and incubated overnight at 4° with antibodies: rαH3 (ab1791, 2 μl/rxn), rαH3K9me3 (39161, 5 μl/rxn, Active Motif, La Hulpe, Belgium) rαH3K27me3 (#17-622, 5 μl/rxn, Merck-Millipore) rαH4K16ac (39167, 4 μl/rxn, Active Motif), rαH3K36me3 (2 μl/rxn, pAb-058–050, Diagenode), rαH3K4me3 (#17-614, 3 μl/rxn, Merck-Millipore) and total IgG (5 μl/rxn, Merck-Millipore). IP was done with 20 μl blocked sepharose A beads/rxn for 90–120 min at 4°C. Beads were washed according to the online available Millipore ChIP protocol (www.millipore.com/techpublications/tech1/mcproto407). DNA was isolated using Chelex 100 resin (Bio-rad) and diluted 1:1 for Q-PCR analysis.

(q)PCR analysis of human subtelomeres. To circumvent potential PCR problems posed by the duplicated and repetitive nature of subtelomeres, we exploited the single copy nature of the subtelomeres of chromosomes 7q and 11q. To quantify histone modifications, we generated primer pairs using Primer3Plus using qPCR settings[44] on both chromosome arms ranging from as close as < 1 kb from the telomere, up to 250 kb from the telomere (**Fig. 2A**). All primer pairs were tested for chromosome specificity using a monochromosomal DNA panel (Coriell). We succeeded to generate specific primers ranging from directly adjacent to the telomere up to 250 kb from the telomere on both the subtelomeres of 7q and 11q. Primer sequences are listed in **Table S1** and annealing temperatures are indicated. q-PCR analysis was done in duplicate using iQ SYBR Green Supermix (Bio-Rad) on the MyIQ thermal cycler or the CFX96^{tm} real time PCR detection system (Bio-Rad) using 4 μl 1:1 diluted ChIP DNA per reaction. Relative quantities of histone modifications were calculated by taking the fold enrichment relative to the IgG background, normalized to input or H3 enrichment: $(Ct_{IgG} - Ct_{modification})/(Ct_{IgG} - Ct_{H3})$. Representative data of 1 of the three culture replicates is shown and error bars indicate SEM of the normalized duplicate q-PCR values.

CpG methylation analysis. CpG islands at TERRA promoters were identified using the CpGplot tool available at www.ebi.ac.uk/Tools/emboss/cpgplot. CpG methylation levels were determined using mass spectrometry based Epityper assays (Sequenom) as described before.[45] In short, DNA is converted with bisulfite and PCR amplified, transcribed to RNA, cleaved by RNaseA and the resulting methylated and unmethylated fragments were quantified by mass spectrometry. All measurements were performed in triplicate. Subtelomeric probe sequences are listed in **Table S1**. The DNA methylation was entered as the dependent to an UNIANOVA (SPSS 18.0), as it accounts for the correlated nature of adjacent CpG sites. Variables defining the cell passage (early and late), the CpG site, the individual triplicates and the genomic location were entered as fixed effects. Data are shown for a single culture experiment; all p-values reported are two-tailed. For **Figures 2D–F and 4B**, the mean methylation level of multiple CpGs within a probe and, for **Figure 2F**, multiple probes per chromosome is displayed.

RNA isolation, TERRA cDNA synthesis and PCR detection. Cells were lysed in QIAzol lysis reagent and subsequently RNA was isolated using the RNeasy mini kit according to manufacturer's instructions (both Qiagen). RNA integrity was confirmed (RIN > 9) by RNA 6000 Nano lab on chip analysis (Agilent technologies) and 2 μg of total RNA was used for TERRA specific cDNA synthesis as described,[23] using the the SuperScript® III First-Strand Synthesis System (Life Technologies). PCR analysis was performed using Phusion® High Fidelity DNA polymerase according to manufacturer's conditions. PCR conditions: initial denaturing: 95°C, 3' followed by 40 cycles of 30'' 95°C, 30'' 60°C (11q, Xq)/61°C (7q), 30'' 72°C and a final extension step of 10' 72°C. Primer sequences are indicated in **Table S1**. PCR products where analyzed by standard 1.5–2% TBE agarose gel electrophoresis and visualized using the OptiGo 750 imaging system with Proxima AQ-4 software (both Isogen life science).

Disclosure of Potential Conflicts of Interest

No potential conflict of interest was disclosed.

Acknowledgments

This study was supported by a grant from the Netherlands Consortium for Healthy Aging (Grant 05060810) in the framework of the Netherlands Genomics Initiative/Netherlands Organization for Scientific Research and the European Union's Seventh Framework Program IDEAL (FP7/2007–2011) under grant agreement nº 259679.

Supplemental Materials

Supplemental materials may be found here:
www.landesbioscience/com/journals/epigenetics/article/24450

References

1. Hayflick L. The limited in vitro lifetime of human diploid cell strains. Exp Cell Res 1965; 37:614-36; PMID:14315085; http://dx.doi.org/10.1016/0014-4827(65)90211-9.
2. de Jesus BB, Blasco MA. Assessing cell and organ senescence biomarkers. Circ Res 2012; 111:97-109; PMID:22723221; http://dx.doi.org/10.1161/CIRCRESAHA.111.247866.
3. Harley CB, Futcher AB, Greider CW. Telomeres shorten during ageing of human fibroblasts. Nature 1990; 345:458-60; PMID:2342578; http://dx.doi.org/10.1038/345458a0.
4. Allsopp RC. Models of initiation of replicative senescence by loss of telomeric DNA. Exp Gerontol 1996; 31:235-43; PMID:8706793; http://dx.doi.org/10.1016/0531-5565(95)02008-X.
5. Vaziri H, Benchimol S. Reconstitution of telomerase activity in normal human cells leads to elongation of telomeres and extended replicative life span. Curr Biol 1998; 8:279-82; PMID:9501072; http://dx.doi.org/10.1016/S0960-9822(98)70109-5.
6. Palm W, de Lange T. How shelterin protects mammalian telomeres. Annu Rev Genet 2008; 42:301-34; PMID:18680434; http://dx.doi.org/10.1146/annurev.genet.41.110306.130350.

7. Demissie S, Levy D, Benjamin EJ, Cupples LA, Gardner JP, Herbert A, et al. Insulin resistance, oxidative stress, hypertension, and leukocyte telomere length in men from the Framingham Heart Study. Aging Cell 2006; 5:325-30; PMID:16913878; http://dx.doi.org/10.1111/j.1474-9726.2006.00224.x.
8. Fitzpatrick AL, Kronmal RA, Gardner JP, Psaty BM, Jenny NS, Tracy RP, et al. Leukocyte telomere length and cardiovascular disease in the cardiovascular health study. Am J Epidemiol 2007; 165:14-21; PMID:17043079; http://dx.doi.org/10.1093/aje/kwj346.
9. Zee RY, Castonguay AJ, Barton NS, Germer S, Martin M. Mean leukocyte telomere length shortening and type 2 diabetes mellitus: a case-control study. Transl Res 2010; 155:166-9; PMID:20303464; http://dx.doi.org/10.1016/j.trsl.2009.09.012.
10. Willeit P, Willeit J, Kloss-Brandstätter A, Kronenberg F, Kiechl S. Fifteen-year follow-up of association between telomere length and incident cancer and cancer mortality. JAMA 2011; 306:42-4; PMID:21730239; http://dx.doi.org/10.1001/jama.2011.901.
11. Aubert G, Lansdorp PM. Telomeres and aging. Physiol Rev 2008; 88:557-79; PMID:18391173; http://dx.doi.org/10.1152/physrev.00026.2007.
12. Benetti R, García-Cao M, Blasco MA. Telomere length regulates the epigenetic status of mammalian telomeres and subtelomeres. Nat Genet 2007; 39:243-50; PMID:17237781; http://dx.doi.org/10.1038/ng1952.
13. Blasco MA. The epigenetic regulation of mammalian telomeres. Nat Rev Genet 2007; 8:299-309; PMID:17363977; http://dx.doi.org/10.1038/nrg2047.
14. Linardopoulou EV, Williams EM, Fan Y, Friedman C, Young JM, Trask BJ. Human subtelomeres are hot spots of interchromosomal recombination and segmental duplication. Nature 2005; 437:94-100; PMID:16136133; http://dx.doi.org/10.1038/nature04029.
15. Ambrosini A, Paul S, Hu S, Riethman H. Human subtelomeric duplicon structure and organization. Genome Biol 2007; 8:R151; PMID:17663781; http://dx.doi.org/10.1186/gb-2007-8-7-r151.
16. Maeda T, Guan JZ, Oyama J, Higuchi Y, Makino N. Age-related changes in subtelomeric methylation in the normal Japanese population. J Gerontol A Biol Sci Med Sci 2009; 64:426-34; PMID:19223605; http://dx.doi.org/10.1093/gerona/gln057.
17. Maeda T, Guan JZ, Koyanagi M, Higuchi Y, Makino N. Aging-associated alteration of telomere length and subtelomeric status in female patients with Parkinson's disease. J Neurogenet 2012; 26:245-51; PMID:22364520; http://dx.doi.org/10.3109/01677063.2011.651665.
18. Guan JZ, Guan WP, Maeda T, Makino N. The Subtelomere of Short Telomeres is Hypermethylated in Alzheimer's Disease. Aging Dis 2012; 3:164-70; PMID:22724077.
19. Gadalla SM, Katki HA, Shebl FM, Giri N, Alter BP, Savage SA. The relationship between DNA methylation and telomere length in dyskeratosis congenita. Aging Cell 2012; 11:24-8; PMID:21981348; http://dx.doi.org/10.1111/j.1474-9726.2011.00755.x.
20. van Overveld PGM, Lemmers RJFL, Sandkuijl LA, Enthoven L, Winokur ST, Bakels F, et al. Hypomethylation of D4Z4 in 4q-linked and non-4q-linked facioscapulohumeral muscular dystrophy. Nat Genet 2003; 35:315-7; PMID:14634647; http://dx.doi.org/10.1038/ng1262.
21. Zeng W, de Greef JC, Chen YY, Chien R, Kong X, Gregson HC, et al. Specific loss of histone H3 lysine 9 trimethylation and HP1gamma/cohesin binding at D4Z4 repeats is associated with facioscapulohumeral dystrophy (FSHD). PLoS Genet 2009; 5:e1000559; PMID:19593370; http://dx.doi.org/10.1371/journal.pgen.1000559.
22. Balog J, Thijssen PE, de Greef JC, Shah B, van Engelen BG, Yokomori K, et al. Correlation analysis of clinical parameters with epigenetic modifications in the DUX4 promoter in FSHD. Epigenetics 2012; 7:579-84; PMID:22522912; http://dx.doi.org/10.4161/epi.20001.
23. Azzalin CM, Reichenbach P, Khoriauli L, Giulotto E, Lingner J. Telomeric repeat containing RNA and RNA surveillance factors at mammalian chromosome ends. Science 2007; 318:798-801; PMID:17916692; http://dx.doi.org/10.1126/science.1147182.
24. Nergadze SG, Farnung BO, Wischnewski H, Khoriauli L, Vitelli V, Chawla R, et al. CpG-island promoters drive transcription of human telomeres. RNA 2009; 15:2186-94; PMID:19850908; http://dx.doi.org/10.1261/rna.1748309.
25. Caslini C, Connelly JA, Serna A, Broccoli D, Hess JL, Caslini C, et al. MLL associates with telomeres and regulates telomeric repeat-containing RNA transcription. Mol Cell Biol 2009; 29:4519-26; PMID:19528237; http://dx.doi.org/10.1128/MCB.00195-09.
26. Deng Z, Wang Z, Stong N, Plasschaert R, Moczan A, Chen HS, et al. A role for CTCF and cohesin in subtelomere chromatin organization, TERRA transcription, and telomere end protection. EMBO J 2012; 31:4165-78; PMID:23010778; http://dx.doi.org/10.1038/emboj.2012.266.
27. Arnoult N, Van Beneden A, Decottignies A. Telomere length regulates TERRA levels through increased trimethylation of telomeric H3K9 and HP1α. Nat Struct Mol Biol 2012; 19:948-56; PMID:22922742; http://dx.doi.org/10.1038/nsmb.2364.
28. Maicher A, Kastner L, Dees M, Luke B. Deregulated telomere transcription causes replication-dependent telomere shortening and promotes cellular senescence. Nucleic Acids Res 2012; 40:6649-59; PMID:22553368; http://dx.doi.org/10.1093/nar/gks358.
29. Pfeiffer V, Lingner J. de (ISREC) SI, Pfeiffer V, Lingner J. TERRA Promotes Telomere Shortening through Exonuclease 1-Mediated Resection of Chromosome Ends. PLoS Genet 2012; 8:1-15; http://dx.doi.org/10.1371/journal.pgen.1002747.
30. Balog J, Miller D, Sanchez-Curtailles E, Carbo-Marques J, Block G, Potman M, et al. Epigenetic regulation of the X-chromosomal macrosatellite repeat encoding for the cancer/testis gene CT47. Eur J Hum Genet 2012; 20:185-91; PMID:21811308; http://dx.doi.org/10.1038/ejhg.2011.150.
31. Chantalat S, Depaux A, Héry P, Barral S, Thuret JY, Dimitrov S, et al. Histone H3 trimethylation at lysine 36 is associated with constitutive and facultative heterochromatin. Genome Res 2011; 21:1426-37; PMID:21803857; http://dx.doi.org/10.1101/gr.118091.110.
32. Dang W, Steffen KK, Perry R, Dorsey JA, Johnson FB, Shilatifard A, et al. Histone H4 lysine 16 acetylation regulates cellular lifespan. Nature 2009; 459:802-7; PMID:19516333; http://dx.doi.org/10.1038/nature08085.
33. Krishnan V, Chow MZ, Wang Z, Zhang L, Liu B, Liu X, et al. Histone H4 lysine 16 hypoacetylation is associated with defective DNA repair and premature senescence in Zmpste24-deficient mice. Proc Natl Acad Sci U S A 2011; 108:12325-30; PMID:21746928; http://dx.doi.org/10.1073/pnas.1102789108.
34. O'Sullivan RJ, Kubicek S, Schreiber SL, Karlseder J. Reduced histone biosynthesis and chromatin changes arising from a damage signal at telomeres. Nat Struct Mol Biol 2010; 17:1218-25; PMID:20890289; http://dx.doi.org/10.1038/nsmb.1897.
35. Chandra T, Kirschner K, Thuret JY, Pope BD, Ryba T, Newman S, et al. Independence of repressive histone marks and chromatin compaction during senescent heterochromatic layer formation. Mol Cell 2012; 47:203-14; PMID:22795131; http://dx.doi.org/10.1016/j.molcel.2012.06.010.
36. Keogh MC, Kurdistani SK, Morris SA, Ahn SH, Podolny V, Collins SR, et al. Cotranscriptional set2 methylation of histone H3 lysine 36 recruits a repressive Rpd3 complex. Cell 2005; 123:593-605; PMID:16286008; http://dx.doi.org/10.1016/j.cell.2005.10.025.
37. Joshi AA, Struhl K. Eaf3 chromodomain interaction with methylated H3-K36 links histone deacetylation to Pol II elongation. Mol Cell 2005; 20:971-8; PMID:16364921; http://dx.doi.org/10.1016/j.molcel.2005.11.021.
38. Carrozza MJ, Li B, Florens L, Suganuma T, Swanson SK, Lee KK, et al. Histone H3 methylation by Set2 directs deacetylation of coding regions by Rpd3S to suppress spurious intragenic transcription. Cell 2005; 123:581-92; PMID:16286007; http://dx.doi.org/10.1016/j.cell.2005.10.023.
39. Baird DM, Rowson J, Wynford-Thomas D, Kipling D. Extensive allelic variation and ultrashort telomeres in senescent human cells. Nat Genet 2003; 33:203-7; PMID:12539050; http://dx.doi.org/10.1038/ng1084.
40. Raz V, Vermolen BJ, Garini Y, Onderwater JJ, Mommaas-Kienhuis MA, Koster AJ, et al. The nuclear lamina promotes telomere aggregation and centromere peripheral localization during senescence of human mesenchymal stem cells. J Cell Sci 2008; 121:4018-28; PMID:19056671; http://dx.doi.org/10.1242/jcs.034876.
41. Ludérus ME, van Steensel B, Chong L, Sibon OC, Cremers FF, de Lange T. Structure, subnuclear distribution, and nuclear matrix association of the mammalian telomeric complex. J Cell Biol 1996; 135:867-81; PMID:8922373; http://dx.doi.org/10.1083/jcb.135.4.867.
42. Cawthon RM. Telomere measurement by quantitative PCR. Nucleic Acids Res 2002; 30:e47; PMID:12000852; http://dx.doi.org/10.1093/nar/30.10.e47.
43. Nelson JD, Denisenko O, Bomsztyk K. Protocol for the fast chromatin immunoprecipitation (ChIP) method. Nat Protoc 2006; 1:179-85; PMID:17406230; http://dx.doi.org/10.1038/nprot.2006.27.
44. Untergasser A, Nijveen H, Rao X, Bisseling T, Geurts R, Leunissen JA. Primer3Plus, an enhanced web interface to Primer3. Nucleic Acids Res 2007; 35(Web Server issue):W71-4; PMID:17485472; http://dx.doi.org/10.1093/nar/gkm306.
45. Tobi EW, Slagboom PE, van Dongen J, Kremer D, Stein AD, Putter H, et al. Prenatal famine and genetic variation are independently and additively associated with DNA methylation at regulatory loci within IGF2/H19. PLoS One 2012; 7:e37933; PMID:22666415; http://dx.doi.org/10.1371/journal.pone.0037933.